

Observational constraints on decaying vacuum dark energy model

Minglei Tong^a and Hyerim Noh^b

Korea Astronomy and Space Science Institute, Daejeon 305-348, Korea

Received: date / Revised version: date

Abstract. The decaying vacuum model (DV), treating dark energy as a varying vacuum, has been studied well recently. The vacuum energy decays linearly with the Hubble parameter in the late-times, $\rho_\Lambda(t) \propto H(t)$, and produces the additional matter component. We constrain the parameters of the DV model using the recent data-sets from supernovae, gamma-ray bursts, baryon acoustic oscillations, CMB, the Hubble rate and x-rays in galaxy clusters. It is found that the best fit of matter density contrast Ω_m in the DV model is much larger than that in Λ CDM model. We give the confidence contours in the $\Omega_m - h$ plane up to 3σ confidence level. Besides, the normalized likelihoods of Ω_m and h are presented, respectively.

PACS. 95.36.+x, 98.80.Cq, 98.80.Es

1 Introduction

Since the observations of the luminosity-redshift relation $d_L(z)$ of type Ia supernovae (SN Ia) indicated that the expansion of the universe is accelerating [1], a cosmic component called dark energy was introduced to explain the acceleration within the framework of general relativity. Whereafter, more and more evidences, such as cosmic microwave background (CMB) [2], large scale structure [3] especially baryon acoustic oscillations (BAO) [4], weak gravitational lensing [5] and x-ray clusters [6, 7], indicated that the universe is spatially flat and dominated by dark energy. A number of dark energy models have been proposed [8], including scalar field [9], vector field [10, 11], holographic dark energy [12], Chaplygin gas [13] and so on. Among them the cosmological constant model (Λ CDM) [14] is the simplest one. However, as well known, the Λ CDM suffers from the fine tuning problem: the observed vacuum energy density of order $\sim 10^{-47} \text{ GeV}^4$ is about 10^{121} orders of magnitude smaller than the value expected by quantum field theory for a cut-off scale being the Plank scale, and is still about 10^{44} orders smaller even for a cut-off scale being the QCD scale [8]. Apart from dark energy models, modified gravity [15, 16] can also explain the acceleration. However, we just focus on dark energy model in this paper.

As an extension to Λ CDM, the the decaying vacuum (DV) dark energy model was proposed [17, 18], based on the incomplete quantum field theory in the curved 4-dimension space-time. In this model, dark energy is described by the varying vacuum, whose energy density decays with the

expansion of the universe leading to an additional production of the matter component. In the late-time with a quasi-de Sitter background, the vacuum density is proportional to the Hubble rate, $\rho_\Lambda(t) \propto H(t)$. However, the equation of state for the vacuum is a constant value $w = p_\Lambda(t)/\rho_\Lambda(t) = -1$, the same as that in the Λ CDM model. Moreover, as a interesting feature, the late-time dynamics of the DV model is similar to Λ CDM [17, 18].

The DV model has been tested by observational data of SN Ia [19], and a joint data from SN Ia, BAO, and CMB [20, 21]. Moreover, the quasar APM 08279+5255 at $z = 3.91$ was used to examine the DV model [22], and it was found that the DV model can greatly alleviate the high redshift cosmic age problem existing in the Λ CDM model. In order to distinguish the DV model from other dark energy models at the late-time Universe, the statefinder and Om diagnostics of the DV model were also presented in [22]. In order to constrain the DV model as completely as possible, besides the observational data of SN Ia of Union2 [23], BAO [25] and CMB [26] used in the recent work [21], we added the data from Gamma-ray bursts (GRBs) at $z > 1.4$ [24], Hubble rate [27, 28] and x-rays in galaxy clusters [7]. The confidence contours in the $\Omega_m - h$ plane with the best fit values of the parameters in the DV model will be given, using various combinations of the data. Furthermore, one-dimension likelihoods of Ω_m and h , respectively, are also analyzed with the corresponding errors up to 3σ .

In the following, we use the unit $8\pi G \equiv c \equiv 1$.

^a mlton@mail.ustc.edu.cn

^b hr@kasi.re.kr

2 The decaying vacuum model

In a spatially flat Friedmann-Lemaitre-Robertson-Walker (FLRW) space-time, the Friedmann equation is

$$\rho_T = 3H^2, \quad (1)$$

where the total energy density $\rho_T = \rho_m + \rho_r + \rho_{DE}$ is composed with matter, radiation and dark energy. $H = \dot{a}/a$ is the Hubble rate of expansion, where an overdot means taking derivative with respect to t , the cosmic time. The dynamic evolution of the total energy density is determined by the following conservation equation

$$\dot{\rho}_T + 3H(\rho_T + p_T) = 0, \quad (2)$$

where p_T stands for the total pressure. For the present epoch, the radiation component can be ignored, and then the Universe only consists of matter (baryons and dark matter) and dark energy. So $\rho_T = \rho_m + \rho_\Lambda$ and $p_T = p_\Lambda$. In the DV model, the vacuum density varies with time, $\rho_\Lambda = \Lambda(t)$, and moreover, the covariance of the Einstein equation demands the equation of state $w = -1$, so $p_\Lambda = -\Lambda(t)$. Thus, Eq. (2) can be written as

$$\dot{\rho}_m + 3H\rho_m = -\dot{\Lambda}(t), \quad (3)$$

showing that the decaying vacuum density $\Lambda(t)$ plays the role of a source for matter production. If Λ is a constant, Eq.(3) reduces to the evolution equation for matter in Λ CDM model. To proceed, one considers the late-time ansatz for DV model [17,18]:

$$\Lambda = \sigma H, \quad (4)$$

where σ is a positive constant. According to Eqs. (1) and (4), σ is determined as $\sigma = 3\Omega_\Lambda H_0$, where Ω_Λ is the present value of the relative dark energy density and $H_0 = 100 h \text{ km s}^{-1} \text{ Mpc}^{-1}$ is the Hubble constant. Combining Eq. (3) and Eq. (4), one can easily get the evolution equation of the Hubble parameter

$$2\dot{H} + 3H^2 - \sigma H = 0, \quad (5)$$

which can be rewritten as

$$2H' + 3H - \sigma = 0, \quad (6)$$

with a prime meaning $' \equiv d/d(\ln a)$. Eq. (6) can be easily resolved to get a solution of the Hubble parameter [17]

$$H = \frac{\sigma}{3} \left(1 + \frac{\Omega_m}{\Omega_\Lambda} a^{-3/2} \right). \quad (7)$$

Therefore, the matter energy density $\rho_m = 3H^2 - \sigma H$ and the vacuum energy density $\Lambda = \sigma H$ have the following explicit forms

$$\rho_m(a) = \frac{\Omega_m^2 \sigma^2}{3\Omega_\Lambda^2 a^3} + \frac{\Omega_m \sigma^2}{3\Omega_\Lambda a^{3/2}}, \quad (8)$$

$$\Lambda(a) = \frac{\sigma^2}{3} + \frac{\Omega_m \sigma^2}{3\Omega_\Lambda a^{3/2}}, \quad (9)$$

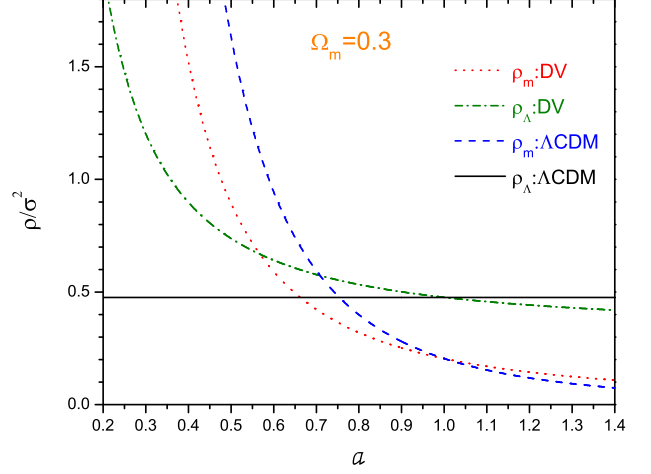


Fig. 1. The dynamic evolutions of the energy density of matter and vacuum in DV model and Λ CDM model, respectively, for a fixed value of the present matter density contrast $\Omega_m = 0.3$.

where we have chosen $a(t_0) = 1$. The first terms in Eqs. (8) and (9) give the usual scaling of the matter and the vacuum, respectively, while the second terms describe the matter production caused by the decaying vacuum. Eqs. (8) and (9) make a smooth transition between the matter and vacuum epochs, which are illustrated in Fig. 1 as an example with $\Omega_m = 0.3$. For comparison, we also plot the cases for Λ CDM. One can see that the equal matter-vacuum dominated epoch in DV model is earlier ($\Delta z \simeq 0.4$) than that in Λ CDM model. From another point of view, the evolution of the Hubble parameter in Eq. (7) as a function of the redshift can be rewritten as

$$H(z) = H_0 [1 - \Omega_m + \Omega_m (1+z)^{3/2}]. \quad (10)$$

Note that, this expression is rather different from that in the standard Λ CDM model, due to the matter production. In particular, if $\Lambda = 0$ and $\Omega_m = 1$, one has $H(z) = H_0 (1+z)^{3/2}$ leading to $\rho_m = 3H_0^2 (1+z)^3$, as expected for the Einstein-de Sitter scenario. On the other hand, if $\Omega_\Lambda = 1$ and $\Omega_m = 0$, we obtain $H(z) = H_0$ and $\Lambda = 3H_0^2$, i.e., the Universe is described by the exact de Sitter space-time and the dark energy density will not vary. In the following, we will discuss the constraints on the DV model using various observational data.

3 Observational constraints

In the following, we use the observational data from SN Ia, BAO, CMB, GRB, Hubble parameter and x-ray in the galaxy clusters to constrain the two free parameters (Ω_m, H_0) of the DV model. As the likelihood function relates to χ^2 function as $\mathcal{L} \propto \exp(-\chi^2/2)$, one should minimize the χ^2 function to obtain the best fit values of the free parameters.

3.1 SN Ia

As did in many literatures, we compare the observed distance modulus $\mu_{obs}(z_i)$ of the 557 SN Ia assembled in the Union2 compilation [23] with the theoretical distance modulus

$$\mu_{th}(z|p_s) = m - M = 5 \log_{10} \frac{d_L}{Mpc} + 25, \quad (11)$$

where m and M are the apparent and absolute magnitudes, respectively, the complete set of parameters is $p_s \equiv (\Omega_m, H_0)$, and

$$d_L(z) = (1+z) \int_0^z \frac{dz'}{H(z')} \quad (12)$$

is the luminosity distance in a spatially flat Universe. For the SN Ia data, the best fit to the set of parameters p_s can be obtained by minimizing the χ^2 function

$$\chi_{SN}^2(p_s) = \sum_{i=1}^{557} \frac{[\mu_{th}(z_i) - \mu_{obs}(z_i)]^2}{\sigma_i^2}, \quad (13)$$

where σ_i stands for the 1σ uncertainty associated with the i th data point.

3.2 GRB

Gamma-ray bursts (GRB) have been proposed to be a complementary probe to SN Ia [29]. Their high energy photons in the gamma-ray band are most intense explosions immune to dust extinction compared to supernovae. So far, there are many GRB observed in the range of $0.1 < z \leq 8.1$, and the maximum redshift of GRB is expected to be 10 or even larger [30]. However, there is a circularity problem in the direct use of GRB [31], mainly due to the lack of a set of low-redshift GRB at $z < 0.1$ which is cosmology-independent. Not only some statistical methods have been proposed to alleviate the circularity problem [32], but also the cosmology-independent method needing a large amount of SN Ia at $z < 1.4$ to calibrate GRB was proposed in [33]. Due to both the significant improvements in GRB and SN Ia, the calibration of GRB was updated [24], which can be used to constrain cosmological models without the circularity problem. The 59 calibrated high-redshift ($z > 1.4$) GRB were obtained with the observed redshift z and modulus μ is shown in Table 2 of Ref. [24]. Hence, the Eq. (13) is also valid for GRB,

$$\chi_{GRB}^2(p_s) = \sum_{i=1}^{59} \frac{[\mu_{th}(z_i) - \mu_{obs}(z_i)]^2}{\sigma_i^2}. \quad (14)$$

3.3 BAO

In the distribution of SDSS luminous red galaxies [34,4] the distance parameter A for the measurement of the BAO

peak has been usually used as a kind of examination in literatures. The definition of A is

$$A \equiv D_V \frac{\sqrt{\Omega_m H_0^2}}{z}, \quad (15)$$

where D_V is the dilation scale, defined as

$$D_V(z) = \left[\frac{z}{H(z)} \left(\int_0^z \frac{dz'}{H(z')} \right)^2 \right]^{1/3}. \quad (16)$$

However, as pointed out in [20], the distance parameter A is not appropriate to test the DV model, since it is obtained from the data in the context of a Λ CDM model and can be considered as a good approximation only for some class of dark energy model [35]. We follow Carneiro et al. [20], using D_V instead which is weakly sensitive to the cosmological evolution before $z = 0.35$. The dilation scale D_V has been observed by the SDSS at $z = 0.35$ [4], as well as by the 2dFGRS at $z = 0.2$ [25]. Moreover, the measurements of SDSS and 2dFGRS yield the ratio $D_V(0.35)/D_V(0.2) = 1.736 \pm 0.065$ [25]. Then the best fit values for the model can be obtained by minimizing [36]

$$\chi_{BAO}^2(p_s) = \frac{([D_V(0.35)/D_V(0.2)]_{th} - [D_V(0.35)/D_V(0.2)]_{obs})^2}{\sigma_{D_V(0.35)/D_V(0.2)}^2}, \quad (17)$$

where $\sigma_{D_V(0.35)/D_V(0.2)}^2 = 0.065$. However, as presented in Ref. [21], it does not impose any constraint on h .

3.4 CMB

The CMB shift parameter defined as [37,38]

$$R \equiv \sqrt{\Omega_m} H_0 \int_0^{z_{rec}} \frac{dz}{H(z)}, \quad (18)$$

with z_{rec} the redshift of recombination, often serves as a contrast in a large class of dark energy models to be compared with that in the Λ CDM model. However, this is only valid if the acoustic horizon at the time of last scattering is the same [39]. This is not true in DV model, as pointed in [20], because for the same values of H_0 and Ω_m we have different expressions for cosmological parameters at high redshifts, due to the process of matter production. In this paper, to employ less fitting expressions, we use the acoustic scale l_A instead of the position for the first peak l_1 in the spectrum of CMB anisotropies [20,21]. The acoustic scale at decoupling epoch is defined as

$$l_A = \frac{\pi \int_0^{z_*} \frac{dz}{H(z)}}{\int_{z_*}^{\infty} \frac{c_s dz}{H(z)}}, \quad (19)$$

where z_* is the redshift of decoupling epoch, and

$$c_s = \left(3 + \frac{9}{4} \frac{\Omega_b}{\Omega_\gamma (1+z)} \right)^{-1/2} \quad (20)$$

is the sound speed of the photon-baryon fluid. Here Ω_b and Ω_γ are the present relative energy densities of baryons and photons. Below, we follow the observational results in [26]: $l_{A,obs} = 302.09$, $z_* = 1091$, $\Omega_b = 0.0455$ and $\Omega_\gamma = 2.469 \times 10^{-5} h^{-2}$ for $T_{CMB} = 2.725 K$. Moreover, at the very early stage for the DV model, the appropriate generalization of Eq. (10) including radiation is given by [20]

$$\frac{H(z)}{H_0} \approx \{[1 - \Omega_m + \Omega_m(1+z)^{3/2}]^2 + \Omega_r(1+z)^4\}^{1/2}, \quad (21)$$

where Ω_r is the present relative energy density of radiation. Here, $\Omega_r = \Omega_\gamma(1 + 0.227 \times N_{eff})$ with Ω_γ the relative energy density of photons and $N_{eff} = 3.04$ the effective number of the standard neutrino species [40]. Therefore, the corresponding χ^2 function is given by

$$\chi_{CMB}^2(p_s) = \frac{(l_{A,th} - l_{A,obs})^2}{\sigma_{l_A}^2}, \quad (22)$$

with $\sigma_{l_A} = 0.76$ [26].

3.5 Hubble rate

Recently, some high precision measurements constrained $H(z)$ at $z = 0$ from the observation of 240 Cepheid variables of rather similar periods and metallicities [27]. The Hubble parameter as a function of redshift can be written as

$$H(z) = -\frac{1}{1+z} \frac{dz}{dt}. \quad (23)$$

Then $H(z)$ is obtained once dz/dt is known. Simon *et al.* [41] and Stern *et al.* [42] obtained $H(z)$ in the range of $0 \leq z \leq 1.8$, using the differential ages of passively-evolving galaxies and archival data. Besides, $H(z)$ at $z = 0.24, 0.34$ and 0.43 is obtained [28] by using the BAO peak position as a standard ruler in the radial direction. We employ the twelve data in [27, 42] and the three data in [28]. The best fit values of the model parameters from observational Hubble data are determined by minimizing

$$\chi_{Hub}^2(p_s) = \sum_{i=1}^{15} \frac{[H_{th}(z_i) - H_{obs}(z_i)]^2}{\sigma^2(z_i)}. \quad (24)$$

3.6 X-rays in galaxy clusters

The baryons in clusters of galaxies are in the form of hot x-ray emitting gas clouds. Thus, the fraction of baryons in clusters, f_{gas} , is defined as the ratio of the x-ray gas mass to the total mass of a gas mass fraction, which is a constant and independent of redshift [43]. Here, we use 42 Chandra measurements of relaxed galaxy clusters in the redshift range $0.05 < z < 0.1$ [7]. To fit the data one can employ the empirical formula [36]

$$f_{gas}(z) = \frac{KA\gamma b(z)}{1 + s(z)} \left(\frac{\Omega_b}{\Omega_m} \right) \left(\frac{d_A^{ACDM}}{d_A} \right)^{3/2}, \quad (25)$$

where the angular correction factor A is approximately given by

$$A \approx \left(\frac{H(z)d_A(z)}{[H(z)d_A(z)]^{ACDM}} \right)^\eta. \quad (26)$$

Here d_A is the angular diameter distance, being related with the luminosity distance by

$$d_A(z) = \frac{d_L(z)}{(1+z)^2}, \quad (27)$$

and the index $\eta = 0.214 \pm 0.022$ [7]. In equation (25), K describes the combined effects of the residual uncertainties such as the instrumental calibration and certain x-ray modelling issues. The parameter γ denotes permissible departures from the assumption of hydrostatic equilibrium due to non-thermal pressure support. The bias $b(z) = b_0(1 + \alpha_b z)$ accounts for uncertainties in the cluster depletion factor, and $s(z)s_0(1 + \alpha_s z)$ answers for uncertainties of the baryonic mass fraction in stars. Most of these parameters have large uncertainties which can be seen in Table 4 in [7]. For simplicity, we fix these parameters in the following: $K = \gamma = 1$, $s_0 = 0.16 h^{1/2}$, $\alpha_s = 0$, $b_0 = 0.835$ [44], and $\alpha_b = 0$. The χ^2 function from x-rays in galaxy clusters is then given by

$$\chi_{x-rays}^2(p_s) = \sum_{i=1}^{42} \frac{([f_{gas}(z_i)]_{th} - [f_{gas}(z_i)]_{obs})^2}{\sigma^2(z_i)}. \quad (28)$$

4 Results and discussions

Based on the discussion above, the total χ^2 is combined as

$$\chi_{total}^2 = \chi_{SN}^2 + \chi_{GRB}^2 + \chi_{BAO}^2 + \chi_{CMB}^2 + \chi_{Hub}^2 + \chi_{x-rays}^2. \quad (29)$$

As the likelihood function is determined as $\mathcal{L} \propto \exp(-\chi^2/2)$, the left panel of Fig.2 shows the 68.3% (1σ), 95.4% (2σ) and 99.7% (3σ) confidence contours of the parameters (Ω_m, h) obtained by various combinations of observational data-sets for the DV model. In order to find how much a set of data contributes to the constraints, we added the sets of data one by one. We can see that the data from CMB and x-rays give very sensitive contributions to the constraints. Here we should emphasize two aspects. Firstly, as discussed in [20], we have used parameters that are strictly correct for the Λ CDM case, which would lead to bias in our results in spite of a good approximation. So, more complete analyses of CMB need to be done. Secondly, as can be seen in Eq. (25), the value of χ_{x-rays}^2 depends on the ratio of the luminosity distances predicted by Λ CDM and ESF, which will deviate from 1 more and more at higher redshift. This is why the result of the best fits is so different with and without the x-rays data. Furthermore, there are many uncertain parameters included in Eq. (25). Different choices of the parameters lead to different contributions from x-ray data to the results. On the other hand, the additions of the data from GRB and

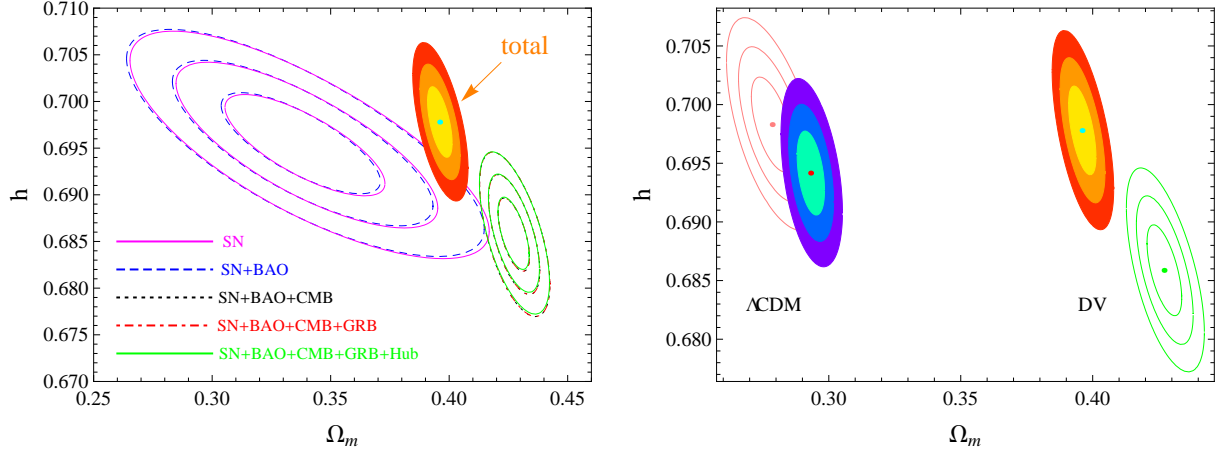


Fig. 2. Left panel: The confidence contours up to 3σ in $\Omega_m - h$ plane for various combinations of observational data. The constraints from total data are shown as shaded contours. Right panel: the constraints for the DV model and Λ CDM model from the total data and the combined data without x-rays, respectively. The solid points stand for the location of the best fit values.

Hubble parameter give negligible influences on the constraints. One can see from Fig. 2 that, the red dash-dotted contours and the black dotted contours overlap with each other, and the green solid contours almost overlap with the previous two sets of contours. Concretely, the best fit values of parameters Ω_m and h with corresponding χ^2_{min} and χ^2_{min}/dof (dof = degrees of freedom) obtained from different combinations of data-sets are presented in Table 1, respectively. In Table 1, we can see that the best fit values of Ω_m and h are very sensitive to the data from CMB and x-rays, but are very insensitive to the data from GRB and Hubble parameter. For comparison, we also give the two cases in the Λ CDM model. A comparison of confidence contours between DV and Λ CDM can be seen in the right panel of Fig. 2. The lined contours are obtained from joint data of SN+BAO+CMB+GRB+Hub, and shaded contours are obtained from the total observational data. The results of the confidence contours obtained without x-rays data, as can be seen in the right panel of Fig. 2 are in good agreement with those appeared in [20,21].

Fig. 3 presents the 1-dimension normalized likelihoods of the two parameters Ω_m and h for DV model based on the total data (blue lines) and the combined data without x-rays (red lines), respectively. Concretely, the best fit values are $\Omega_m = 0.3960^{+0.0034}_{-0.0033}(1\sigma)^{+0.0070}_{-0.0067}(2\sigma)^{+0.0104}_{-0.0099}(3\sigma)$ and $h = 0.6978 \pm 0.0025 \pm 0.0050 \pm 0.0074$ with $\chi^2_{total} = 966.343$. If we abandon the data from x-ray, the best fit values are $\Omega_m = 0.4270^{+0.0044+0.0089+0.0132}_{-0.0043-0.0085-0.0125}$ and $h = 0.6858 \pm 0.0025 \pm 0.0050^{+0.0076}_{-0.0075}$ with $\chi^2_{total} = 596.345$. One can see the big different results of the both likelihoods of Ω_m and h . As discussed above, the differences are due to the deviations of the luminosity distance given by ESF from that given by Λ CDM.

Just as the results from the examination using energy density perturbations [45], the best fits of Ω_m for DV model are very large compared to those for Λ CDM

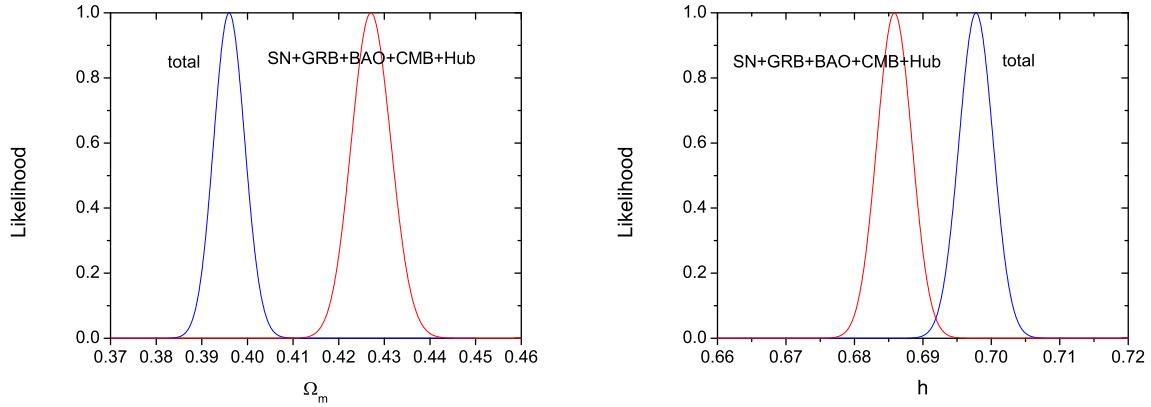
model. The data from CMB give a magnificent response for the large value of Ω_m . However, more complete analyses of CMB need to be done. Moreover, there are many parameters with large uncertainties in Eq. (25), when we evaluate χ^2_{x-rays} in Eq. (28). This defect can just explain the large value of $\chi^2_{min}/dof = 1.44$, which can be seen in Table 1.

5 Conclusions

We constrained the parameters of the DV model using the most recent joint data from 557 SN Ia in Union2 compilation, 59 GRBs in the high redshifts ($z > 1.4$), the ratio of the dilation scale at $z = 0.35$ and $z = 0.2$ of BAO, the acoustic scale at decoupling epoch of CMB measured by WMAP 7, 15 data of Hubble rate, and 42 x-ray gas mass ratio in galaxy clusters. Due to the joint data, the parameters of the best fit values are: $\Omega_m = 0.3960^{+0.0034+0.0070+0.0104}_{-0.0033-0.0067-0.0099}$ and $h = 0.6978 \pm 0.0025 \pm 0.0050 \pm 0.0074$. With the same joint data, we also calculated the best fits for Λ CDM model: $\Omega_m = 0.2931^{+0.0034+0.0069+0.0104}_{-0.0034-0.0067-0.0099}$ and $h = 0.6941 \pm 0.0024 \pm 0.0047 \pm 0.0070$. However, the data from x-rays depend on many fitting parameters with a large uncertainty. Then, if we neglect the poor data of x-rays, the results are: $\Omega_m = 0.4270^{+0.0044+0.0089+0.0132}_{-0.0043-0.0085-0.0125}$ and $h = 0.6858 \pm 0.0025 \pm 0.0050^{+0.0076}_{-0.0075}$ for the DV model; $\Omega_m = 0.2785^{+0.0054+0.0109+0.0164}_{-0.0052-0.0103-0.0151}$ and $h = 0.6983 \pm 0.0027 \pm 0.0053 \pm 0.0079$ for the Λ CDM model. The best fit value of Ω_m in the DV model is larger than that in the Λ CDM model, since there is additional production of the matter component due to the decaying of the vacuum energy. However, we cannot rule out the DV model from the current observational data. We should wait for more abundant, accurate, and model-independent data to constrain this model. On the other hand, the DV model alleviates

Table 1. The best fit values of the DV model using different combinations of data-sets.

Data	Ω_m	h	χ^2_{min}	χ^2_{min}/dof
SN	0.3388	0.6953	544.587	0.98
SN+BAO	0.3369	0.6955	545.758	0.98
SN+BAO+CMB	0.4272	0.6857	561.724	1.01
SN+BAO+CMB+GRB	0.4272	0.6857	584.866	0.95
SN+BAO+CMB+GRB+Hub	0.4271	0.6859	596.345	0.95
total	0.3960	0.6978	966.343	1.44
SN+BAO+CMB+GRB+Hub (Λ CDM)	0.2785	0.6983	577.915	0.92
total (Λ CDM)	0.2931	0.6941	632.412	0.94

**Fig. 3.** The normalized likelihoods of the parameters Ω_m and h , respectively, for the DV model.

the fine tuning problem and high redshift cosmic age problem which exist in Λ CDM model.

ACKNOWLEDGMENT: H. Noh's work has been supported by Mid-career Research Program through National Research Foundation funded by the MEST (No. 2010-0000302).

References

1. A.G. Riess et al., *Astron. J.* **116**, 1009 (1998);
A.G. Riess et al., *Astrophys. J.* **117**, 707 (1999);
S. Perlmutter et al., *Astrophys. J.* **517**, 565 (1999).
2. C.L. Bennett et al., *Astrophys. J. Suppl.* **148**, 1 (2003);
D.N. Spergel et al., *Astrophys. J. Suppl.* **148**, 175 (2003);
H. V. Peiris et al., *Astrophys. J. Suppl.* **148**, 213 (2003);
D.N. Spergel et al., *Astrophys. J. Suppl.* **170**, 377 (2007);
L. Page et al., *Astrophys. J. Suppl.* **170**, 335 (2007);
G. Hinshaw et al., *Astrophys. J. Suppl.* **170**, 263 (2007);
G. Hinshaw et al., *Astrophys. J. Suppl.* **180**, 225 (2009);
M.R.olta et al., *Astrophys. J. Suppl.* **180**, 296 (2009);
J. Dunkley et al., *Astrophys. J. Suppl.* **180**, 306 (2009);
E. Komatsu et al., *Astrophys. J. Suppl.* **180**, 330 (2009).
3. N.A. Bahcall, J.P. Ostriker, S. Perlmutter, P.J. Steinhardt, *Science* **284**, 1481 (1999).
4. D.J. Eisenstein et al., *Astrophys. J.* **633**, 560 (2005).
5. J. Jarvis, B. Jain, G. Bernstein, D. Dolney, *Astrophys. J.* **644**, 71 (2006);
H. Heikstra et al., *Astrophys. J.* **647**, 116 (2006);
R. Massey et al., *Nature* **445**, 286 (2007).
6. S.W. Allen et al., *Mon. Not. Roy. Astron. Soc.* **353**, 457 (2004).
7. S.W. Allen et al., *Mon. Not. Roy. Astron. Soc.* **383**, 879 (2008).
8. E.J. Copeland, M. Sami, S. Tsujikawa, *Int. J. Mod. Phys. D* **15** 1753 (2006).
9. B. Ratra, P.J.E Peebles, *Phys. Rev. D* **37** 3406 (1988);
I. Zlatev, L.M Wang, P.J. Steinhardt, *Phys. Rev. Lett.* **82**, 896 (1999);
P.J. Steinhardt, L. Wang, I. Zlatev, *Phys. Rev. D* **59**, 123504 (1999);
P.G. Ferreira, M. Joyce, *Phys. Rev. D* **58**, 023503 (1998);
S. Dodelson, M. Kaplinghat, E. Steinhardt, *Phys. Rev. Lett.* **85**, 5276 (2000);
F.C. Carvalho, J.S. Alcaniz, J.A.S. Lima, R. Silva, *Phys. Rev. Lett.* **97**, 081301 (2006);
M.L. Tong, Y. Zhang, Z.W. Fu, *Class. Quantum Grav.* **28**, 055006 (2011).
10. Y. Zhang, *Phys. Lett. B* **340** 18 (1994);
Y. Zhang, *Gen. Relativ. Gravit.* **34**, 2155 (2002);
Y. Zhang, *Gen. Relativ. Gravit.* **35**, 689 (2003);
W. Zhao, Y. Zhang, *Phys. Lett. B* **690**, 64 (2006);
Y. Zhang, T.Y. Xia, W. Zhao, *Class. Quantum Grav.* **24**, 3309 (2007);

- T.Y. Xia, Y. Zhang, Phys. Lett. B **656**, 19 (2007);
M.L. Tong, Y. Zhang, T.Y. Xia, Int. J. Mod. Phys. D **18**, 797 (2009).
11. V.V. Kiselev, Class. Quantum Grav. **21**, 3323 (2004);
C. Armendariz-Picon, JCAP **07**, 007 (2004).
 12. A.G. Cohen, D.B. Kaplan, A.E. Nelson, Phys. Rev. Lett. **82**, 4971 (1999);
D. Pavón, W. Zimdahl, Phys. Lett. B **628**, 206 (2005);
M. Li, Phys. Lett. B, **603** 1 (2004).
C. Gao, F. Wu, X. Chen, Phys. Rev. D **79**, 043511 (2009).
 13. A.Y. Kamenshchik, U. Moschella, V. Pasquier, Phys. Lett. B, **511**, 265(2001);
M.C. Bento, O. Bertolami, A.A. Sen, Phys. Rev. D **66**, 043507 (2002).
 14. S. Weinberg, Rev. Mod. Phys. **61**, 1 (1989);
T. Padmanabhan, Phys. Rep. **380**, 235 (2003).
 15. L.Parker, A. Raval, Phys. Rev. D **60**, 063512 (1999); Phys. Rev. D **60**, 123502 (1999);
S.M. Carroll, V. Duvvuri, M. Trodden, M.S. Turner Phys. Rev. D **70**, 043528 (2004).
 16. M. Trodden, arXiv:1011.0861;
V.T. Toth. arXiv:1011.5174.
 17. H.A. Borges, S. Carneiro, Gen. Relativ. Gravit. **37**, 1385 (2005).
 18. S. Carneiro, J. Phys. A **40**, 6841 (2007).
 19. S. Carneiro, C. Pigozzo, H.A. Borges, J.S. Alcaniz, Phys. Rev. D **74**, 023532 (2006).
 20. S. Carneiro, M.A. Dantas, C. Pigozzo, J.S. Alcaniz, Phys. Rev. D **77**, 083504 (2008).
 21. C. Pigozzo, M. A. Dantas, S. Carneiro, J. S. Alcaniz, arXiv:1007.5290.
 22. M.L. Tong, Y. Zhang, Phys. Rev. D **80**, 023503.
 23. R. Amanullah, et al., Astrophys. J. **716**, 712 (2010).
 24. H. Wei, JCAP **08**, 020 (2010).
 25. W.J. Percival et al., Mon. Not. R. Astron. Soc. **401**, 2148 (2010).
 26. Komatsu et al., arXiv:1001.4538.
 27. A.G. Riess et al., Astrophys. J. **659**, 98 (2007).
 28. E. Gaztañaga, A. Cabré, L. Hui, Mon. Not. R. Astron. Soc. **399**, 1663 (2009).
 29. B.E. Schaefer, Astrophys. J. **660**, 16 (2007).
 30. V. Bromm, A. Loeb, Astrophys. J. **575**, 111 (2002);
J.-R. Lin, S.N. Zhang, T.P. Li, Astrophys. J. **605**, 819 (2004).
 31. G. Ghirlanda, G. Ghisellini, C. Firmani, New. J. Phys. **8**, 123, (2008).
 32. G. Ghirlanda, G. ghisellini, D. lazzati, C. firmani, Astrophys. J. **613**, L13, (2004);
C. Firmani, G. ghisellini, G. Ghirlanda, V. Avila-Reese, Mon. Not. Roy. Astron. Soc. **360**, L1, (2005);
H. Li et al., Astrophys. J. **680**, 92 (2008);
E.-W. Liang, B. Zhang, Mon. Not. Roy. Astron. Soc. Lett. **369**, L37 (2006).
 33. N. Liang, W.K. Xiao, Y. Liu, S.N. Zhang, Astrophys. J. **685**, 354 (2008).
 34. M. Tegmark et al., Phys. Rev. D **69**, 103501, (2004).
 35. M. Doran, S. Stern, E. Thommes, JCAP **04**, 015 (2007).
 36. I. Durán, D. Pavón, W. Zimdahl, JCAP **07**, 018 (2010);
L.X. Xu, J.B. Lu, JCAP **03**, 025 (2010).
 37. J.R. Bond, G. Efsthioiu, M. Tegmark, Mon. Not. Roy. Astron. Soc. **291**, L33 (1997).
 38. Y. Wang, P. Mukherjee, Astrophys. J. **650**, 1 (2006).
 39. O. Elgaroy, T. Multamaki, Astron. Astrophys. **471**, 65 (2007).
 40. G. Mangano, et al., Nucl. Phys. B **729**, 221 (2005).
 41. J. Simon, L. Verde, R. Jiménez, Phys. Rev. D **71**, 123001 (2005).
 42. D. Stern, R. Jiménez, L. Verde, M. Kamionkowski, S.A. Stanford, JCAP **02**, 008 (2010).
 43. S.M.D. White, J.F. Navarro, A. Evrard, C.S. Frenk, Nature **366**, 429 (1993).
 44. V.R. Eke, J.F. Navarro, C.S. Frenk, Astrophys. J. **503**, 569 (1998);
R.A. Crain, et al., Mon. Not. Roy. Astron. Soc. **377**, 41 (2007).
 45. H.A. Borges, S. Carneiro, J.C. Fabris, Phys. Rev. D **78**, 123522 (2008).